J Appl Electrochem (2008) 38:885–891
DOI 10.1007/s10800-008-9493-7

ORIGINAL PAPER

# Thermodynamic and kinetic aspects of the electron transfer reaction of bovine cytochrome *c* immobilized on 4-mercaptopyridine and 11-mercapto-1-undecanoic acid films

**Stefano Monari · Gianantonio Battistuzzi · Marco Borsari · Diego Millo · Cees Gooijer · Gert van der Zwan · Antonio Ranieri · Marco Sola**

Received: 13 September 2007 / Revised: 7 January 2008 / Accepted: 17 January 2008 / Published online: 5 February 2008
© Springer Science+Business Media B.V. 2008

**Abstract** Bovine cytochrome *c* (cyt *c*) was adsorbed on a polycrystalline gold electrode coated with 4-mercaptopyridine and 11-mercapto-1-undecanoic acid self-assembled monolayers (SAMs) and the thermodynamics and kinetics of the heterogeneous protein-electrode electron transfer (ET) reaction were determined by cyclic voltammetry. The $E^{\circ\prime}$ values for the immobilized protein were found to be lower than those for the corresponding diffusing species. The thermodynamic parameters for protein reduction ($\Delta H^{\circ\prime}_{rc}$ and $\Delta S^{\circ\prime}_{rc}$) indicate that the stabilization of the ferric state due to protein–SAM interaction is enthalpic in origin. The kinetic data suggest that a tunneling mechanism is involved in the ET reaction: the distance between the redox center of the protein and the electrode surface can be efficiently evaluated using the Marcus equation.

**Keywords** Electron transfer · Bovine cytochrome *c* · Redox potential · Cyclic voltammetry · Surface immobilization · Self assembled monolayers

## 1 Introduction

Cytochrome *c* is an important heme-protein characterized by two redox states ($Fe^{3+}/Fe^{2+}$) which is involved in the electron transfer (ET) chains of respiratory processes [1, 2]. The redox chemistry of the freely diffusing protein has been thoroughly investigated by voltammetry in the last two decades [3–8]: these studies enlighted the molecular determinants of the redox potential ($E^{\circ\prime}$) and how the ET reaction is affected by temperature, ionic strength, pH-induced conformational changes, nature of the solvent and ligand binding. Recently, ET processes have been observed for cytochrome *c* (cyt *c*) adsorbed in non-denaturing conditions on bare or functionalized solid electrodes through covalent linkages or electrostatic interactions, respectively [9–24]. This kind of investigation can contribute to the comprehension of the mechanism of ET between protein partners and is a key step for the assembly of biomolecular electronic devices [25].

The mechanism by which cyt *c* exchanges electrons with the partner proteins is a fundamental issue. The most likely electron pathway involves the small portion of the heme which is accessible to the solvent [26]. The heme edge is surrounded by a number of surface lysines which create a positive electrostatic potential functional to the recognition of the complementary domain in the ET partner [1, 2, 27]. Therefore, protein voltammetry of cyt *c* chemisorbed on a solid (gold) electrode coated with negatively charged self-assembled monolayers (SAMs) offers a powerful tool for investigating the kinetic and thermodynamic aspects of physiological ET [11–14, 17–22]. In fact, the suitable choice of the SAM components and of protein variants (or chemically modified derivatives) allows information to be gained on the influence of the distance between the ET centers, nature of the intervening medium and heme orientation on the ET reaction.

Here, we have exploited this approach on bovine cyt *c* chemisorbed onto an uncharged SAM made of 4-mercaptopyridine and on a negatively charged SAM made of

S. Monari · G. Battistuzzi · M. Borsari (✉) · A. Ranieri · M. Sola
Department of Chemistry, University of Modena and Reggio Emilia, Via Campi 183, 41100 Modena, Italy
e-mail: borsari.marco@unimore.it

D. Millo · C. Gooijer · G. van der Zwan
Laser Centre – Analytical Chemistry and Applied Spectroscopy, Vrije Universiteit Amsterdam, De Boelelaan 1081, 1081 HV Amsterdam, The Netherlands

11-mercapto-1-undecanoic acid both anchored to a polycrystalline gold surface. In both cases densely packed layers able to provide a strong interfacial binding to cyt *c* and a fast ET can be obtained [11–14, 17–22, 28–30]. We have chosen these two thiols as SAM constituents because the resulting layers feature remarkable differences in structure and interaction properties toward cyt *c*. This is functional to gaining information on the electron tunnelling process from the protein to the electrode across different monolayers.

The enthalpy and entropy changes of the redox reaction were determined from variable temperature $E^{\circ\prime}$ measurements: these parameters help the comprehension of the molecular changes affecting the redox reaction. Moreover, the rate constants of heterogeneous ET were measured which, within the frame of the Marcus theory, allow insight to be gained on the distance and reorganization energy and therefore on the geometric features of the protein–SAM interaction.

## 2 Experimental

### 2.1 Materials

All chemicals were of reagent grade. Bovine cyt *c* was purchased from Sigma-Aldrich. 11-mercapto-1-undecanoic acid (Sigma-Aldrich) and 4-mercaptopyridine (Sigma-Aldrich) were re-crystallized from hexane before use. Nanopure water was used throughout.

### 2.2 Electrochemical measurements

Cyclic voltammetry (CV) experiments were carried out with a Potentiostat/Galvanostat PAR mod. 273A at different scan rates (0.02–10 V $s^{-1}$) using a cell for small volume samples (0.5 mL) under argon. Experiments on immobilized cyt *c* were carried out using a 1 mm-diameter polycrystalline gold wire as working electrode; a Pt sheet and a saturated calomel electrode (SCE) were used as counter and reference electrode, respectively. The electric contact between the SCE and the working solution was obtained with a Vycor® set. Potentials were calibrated against the $MV^{2+}/MV^{+}$ couple (MV = methylviologen). All the redox potentials reported here are referred to SHE. The working gold electrode was cleaned by dipping it in concentrated nitric acid for 10 min, then flaming it in oxidizing conditions. Afterwards, it was heated in concentrated KOH for 4 h then, after rinsing in water, in concentrated sulfuric acid for 12 h. To minimize residual adsorbed impurities, the electrode was first set at −0.7 V (vs. SCE) for 200 s in 5 mM $NaClO_4$, then subjected to 10 voltammetric cycles between +0.7 and −0.6 V (vs. SCE) at 0.1 V $s^{-1}$; finally the electrode was rinsed in water and anhydrous ethanol. Vycor® (PAR) set was treated in an ultrasonic pool for about 5 min. The 11-mercapto-1-undecanoic acid SAM (MUA, here after) covalently attached onto the gold electrode was obtained by dipping the polished electrode into a 1 mM ethanolic solution of the molecule for 48 h and then rinsing it with MILLIQ water. Protein solutions were freshly prepared before use in 5 mM phosphate buffer at pH = 7 and their concentration (typically 0.2 mM) was checked spectrophotometrically. The 4-mercaptopyridine SAM (MP, here after) was performed by dipping the polished electrode into a 1 mM aqueous solution of the molecule for 5 min, then rinsing it with nanopure water. Protein adsorption on both the SAM-coated Au electrodes was achieved dipping the functionalized electrode into a 0.2 mM protein solution at 4 °C for 4 h. 5 mM sodium perchlorate and 5 mM phosphate buffer at pH = 7 were used as the base electrolyte. The formal reduction potentials $E^{\circ\prime}$ for cyt *c* were calculated from the average of the anodic and cathodic peak potentials. This is appropriate since $\alpha$ is found to be approximately 0.5 and $E^{\circ\prime}$ is almost independent of the scan rate in the range 0.02–10 V $s^{-1}$ [12, 31, 38–41]. The experiments were performed at least two times and the reduction potentials were found to be reproducible within ±2 mV. Cyclic voltammograms at variable scan rate were also recorded in order to determine the ET rate constant $k_s$ for the adsorbed protein. $k_s$ values were averaged over five measurements and found to be reproducible within 6%, which was taken as the associate error. The CV experiments at different temperatures were carried out with a cell in a "nonisothermal" setting [31, 32], namely in which the reference electrode is kept at constant temperature (21 ± 0.1 °C) whereas the half-cell containing the working electrode and the Vycor® junction to the reference electrode is under thermostatic control with a water bath. The temperature was varied from 5 to 45 °C. With this experimental configuration, the reaction entropy for protein reduction ($\Delta S^{\circ\prime}_{rc}$) is given by [31–33]:

$$\Delta S^{\circ\prime}_{rc} = S^{\circ\prime}_{red} - S^{\circ\prime}_{ox} = nF\frac{dE^{\circ\prime}}{dT} \quad (1)$$

thus, $\Delta S^{\circ\prime}_{rc}$ was determined from the slope of the plot of $E^{\circ\prime}$ vs. temperature which turns out to be linear under the assumption that $\Delta S^{\circ\prime}_{rc}$ is constant over the limited temperature range investigated. With the same assumption, the enthalpy change ($\Delta H^{\circ\prime}_{rc}$) was obtained from the Gibbs-Helmholtz equation, namely as the negative slope of the $E^{\circ\prime}/T$ vs. $1/T$ plot. The nonisothermal behavior of the cell was carefully checked by determining the $\Delta H^{\circ\prime}_{rc}$ and $\Delta S^{\circ\prime}_{rc}$ values of the ferricyanide/ferrocyanide couple [31, 32, 34].

## 3 Results

The voltammetric responses of cyt *c* adsorbed on MUA and MP are shown in Fig. 1.

In both the cases, the CV signal shows two well-defined current peaks corresponding to the one-electron reduction/oxidation of adsorbed cyt *c*. Independently of the nature of the SAM, the peak current values were found to be linear with scan rate and almost independent of temperature in the range 5–35 °C (not shown). At higher temperature, the peak current decreases and at 55 °C the CV signals disappear. Formal reduction potentials $E^{\circ\prime}\left(=\frac{E_{pc}+E_{pa}}{2}\right)$ of +195 and +203 mV ($T = 20$ °C) were determined for MUA and MP, respectively (Table 1). The $E^{\circ\prime}$ values are scan rate-independent from 0.020 to 10 V $s^{-1}$.

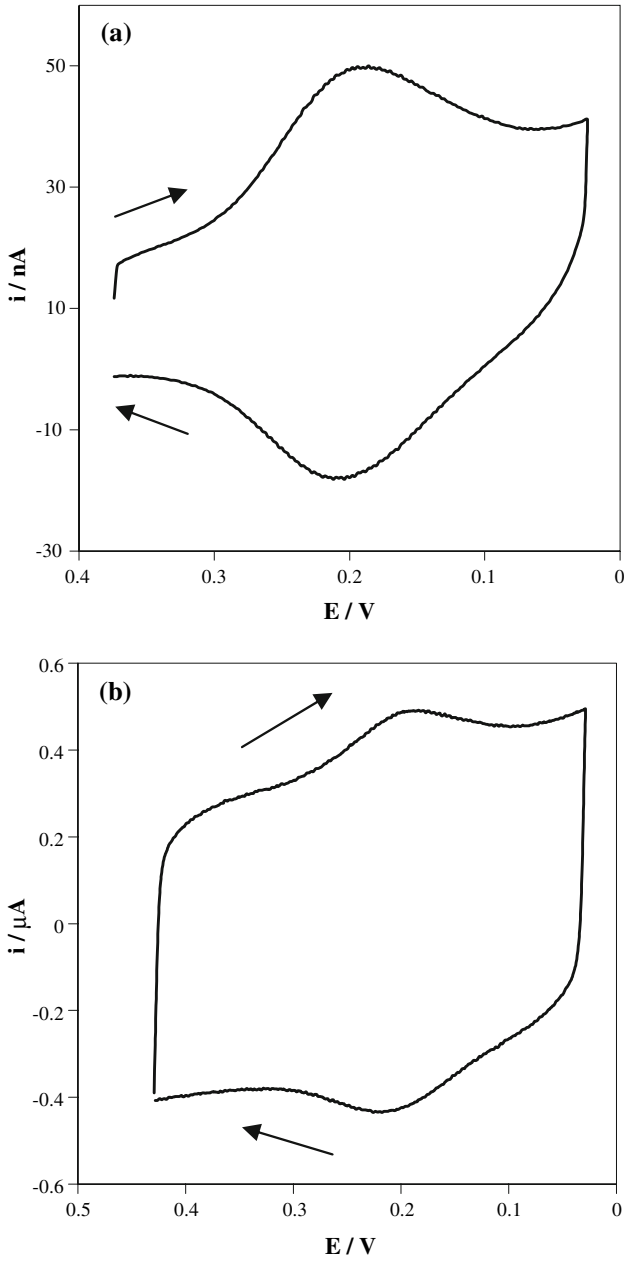


**Fig. 1** Cyclic voltammograms for bovine cyt *c* adsorbed on MUA (**a**) and MP (**b**). Scan rate = 50 mV $s^{-1}$; working solution: 5 mM sodium perchlorate, 5 mM phosphate buffer, pH = 7, $T = 15$ °C

The temperature dependence of $E^{\circ\prime}$ for cyt *c* adsorbed on MUA and MP is illustrated in Fig. 2. The $E^{\circ\prime}$ values show a monotonic linear decrease with increasing temperature from 5 to 35–45 °C.

Figure 3 shows the Gibbs-Helmholtz plots ($E^{\circ\prime}/T$ vs. $1/T$). The reduction entropy and enthalpy values obtained for the different surfaces are listed in Table 1.

Surface coverage of cyt *c* on MUA and MP, calculated from the overall charge exchanged (determined upon integration of the baseline-corrected anodic or cathodic peaks) and the area of the gold electrode (determined from the diffusion controlled CV of the electrochemical standard ferricinium tetrafluoboride in water), are listed in Table 1. The protein coverage on MUA turn out to be very similar to that expected for a full densely packed monolayer, which amounts to 19 pmol $cm^{-2}$, as estimated from the crystallographic dimensions of the protein [15, 27]. In the case of MP, instead, the coverage is lower.

The rate constants for the ET between the heme group of the protein adsorbed on MUA and MP and the electrode, $k_s$ (Table 2), were determined from the scan rate dependence of the anodic and cathodic peak potentials (Fig. 4), following Laviron's model for diffusionless electrochemical systems [35].

Table 2 also lists the activation enthalpies ($\Delta H^{\#}$) calculated from the $k_s$ values using the Arrhenius equation:

$$k_s = A' \exp\left(\frac{-\Delta H^{\#}}{RT}\right) \quad (2)$$

namely from the slope of the ln $k_s$ vs. $1/T$ (Fig. 5).

**Table 1** Reduction thermodynamics and surface coverage for bovine cyt *c* on different SAMs[a]: 4-mercaptopyridine (MP), 11-mercapto-1-undecanoic acid (MUA), 11-mercapto-1-undecanol (MU)

| | MP | MUA | MU[b] | Solution[c] |
|---|---|---|---|---|
| $E^{\circ\prime}$/mV | +203 | +195 | +219 | +275 |
| $\Delta S^{\circ\prime}_{rc}$/J $mol^{-1}$ $K^{-1}$ | −74 | −73 | −45 | −28 |
| $\Delta H^{\circ\prime}_{rc}$/kJ $mol^{-1}$ | −40.8 | −40.1 | −34.2 | −34.7 |
| $(-\Delta\Delta H^{\circ\prime}_{rc,el}/F)$/mV | −72 | −80 | −56 | – |
| $\Gamma^{cyt}_{max}$/pmol $cm^{-2}$ | 12.5 | 18.9 | 6.5 | – |

[a] Working solution: 5 mM sodium perchlorate, 5 mM phosphate buffer, pH = 7, $T = 20$ °C. Average errors on $E^{\circ\prime}$, $\Delta S^{\circ\prime}_{rc}$, $\Delta H^{\circ\prime}_{rc}$, $(-\Delta\Delta H^{\circ\prime}_{rc,el}/F)$ and $\Gamma^{cyt}_{max}$ values are ±2 mV, ±2 J $mol^{-1}$ $K^{-1}$, ±0.3 kJ $mol^{-1}$, ±4 mV, ±5%, respectively

[b] From Ref. [38]

[c] Values determined for the freely diffusing protein in the same conditions (from Ref. [38])

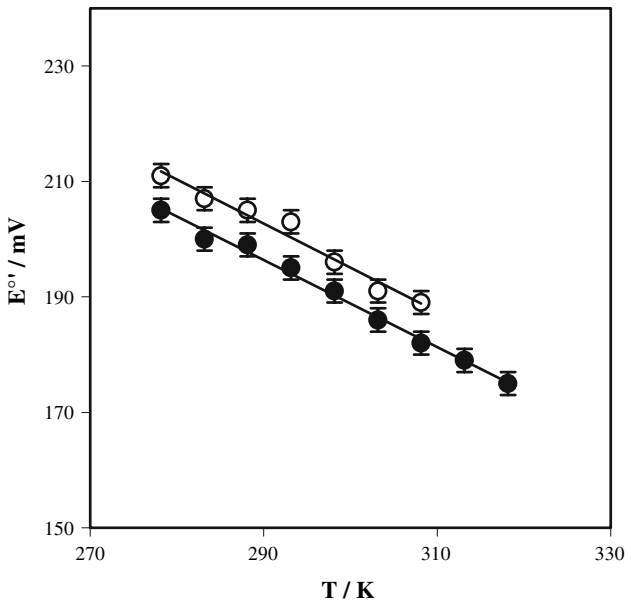


**Fig. 2** $E^{\circ\prime}$ vs. $T$ plots for bovine cyt $c$ adsorbed on MUA (●) and MP (○). Working solution: 5 mM sodium perchlorate, 5 mM phosphate buffer, pH = 7

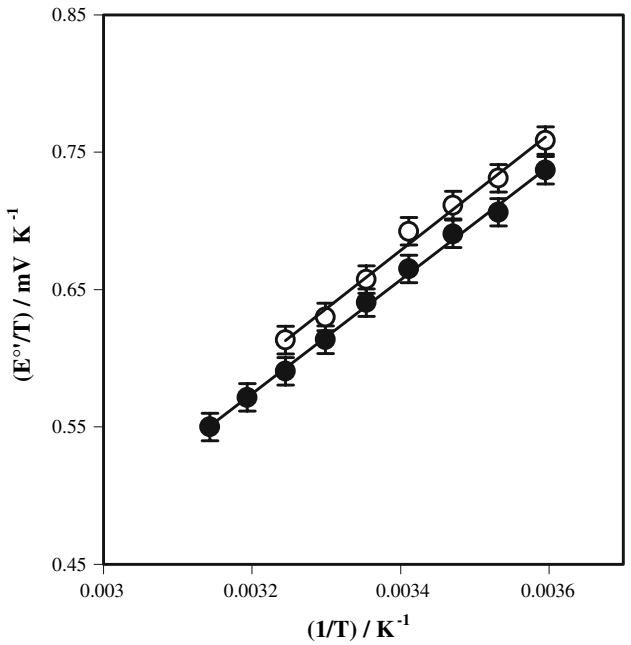


**Fig. 3** $E^{\circ\prime}/T$ vs. $1/T$ plots for bovine cyt $c$ adsorbed on MUA (●) and MP (○). Working solution: 5 mM sodium perchlorate, 5 mM phosphate buffer, pH = 7

## 4 Discussion

The $E^{\circ\prime}$ values for bovine cyt $c$ adsorbed on MUA and MP are lower than that for the protein in solution by 80 and 72 mV (at 20 °C), respectively (Table 1). These differences are similar to those previously reported for the same species chemisorbed on carboxylalkanethiolate SAMs [10–14, 17–22]. This effect can be attributed to the selective stabilization of the (more positively charged) oxidized state over the reduced state of the immobilized cyt $c$ induced by the electrostatic interaction with negative charges of the 11-mercapto-1-undecanoic acid layer and to the H-bonding network formed with the 4-mercaptopyridine surface, respectively [10]. The difference between the $E^{\circ\prime}$ for cyt $c$ adsorbed on MP bound to Au ($E^{\circ\prime}$ = +203 mV) and MP bound to Ag ($E^{\circ\prime}$ = +181 mV) [36] can be, at least in part, attributed to the different experimental conditions employed. Indeed, 5 mM $NaClO_4$ plus 5 mM phosphate buffer and 10 mM phosphate buffer plus 10 mM $Na_2SO_4$ were used as supporting electrolyte on the Au and Ag electrode, respectively [36]. However, the topography of the electrode surface could also contribute to the observed difference. In fact, the surface roughness has been proposed to influence the ability of the protein to exchange electrons

**Table 2** $k_s$ (20 °C), $\Delta H^{\#}$ and $\lambda$ values for bovine cyt $c$ adsorbed on different SAMs[a]

| Surface | $k_s/s^{-1}$ | $\Delta H^{\#}$/kJ mol$^{-1}$ | $\lambda$/eV |
|---|---|---|---|
| MP | 29 | 8.3 | 0.34 |
| MUA | 24 | 5.9 | 0.25 |

[a] Working solution: 5 mM sodium perchlorate, 5 mM phosphate buffer, pH = 7. Average errors on $k_s$, $\Delta H^{\#}$, and $\lambda$ values are ±6%, ±0.3 kJ mol$^{-1}$, ±0.03 eV, respectively

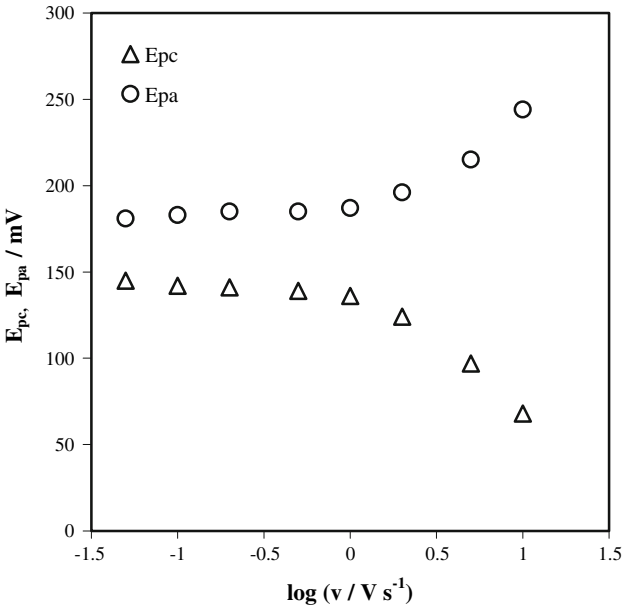


**Fig. 4** Scan rate dependence of the anodic ($E_{pa}$) and cathodic ($E_{pc}$) peak potentials for bovine cyt $c$ adsorbed on MP. Working solution: 5 mM sodium perchlorate, 5 mM phosphate buffer, pH = 7, $T$ = 15 °C. The corresponding data obtained on MUA are closely similar

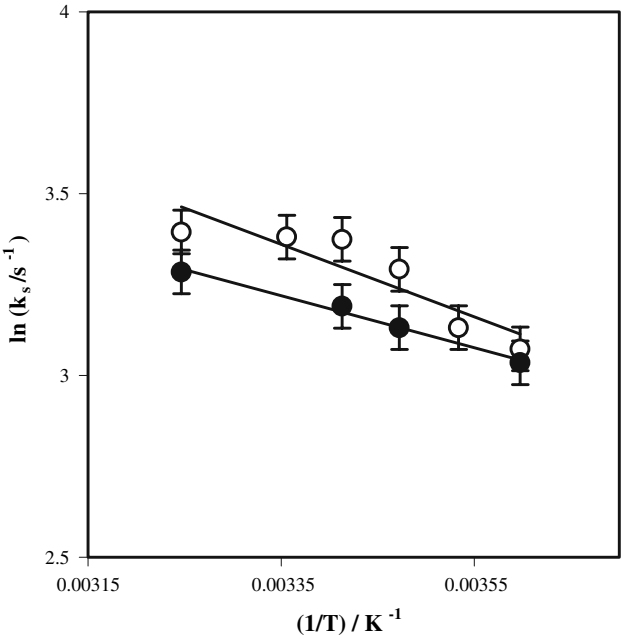


**Fig. 5** ln $k_s$ vs. $1/T$ plots for bovine cyt *c* adsorbed on MUA (●) and MP (○). Working solution: 5 mM sodium perchlorate, 5 mM phosphate buffer, pH = 7

with both Au [37] and Ag [36] electrodes through the SAM.

MP interacts weakly with cyt *c* through H-bond networks involving the pyridine nitrogen and, possibly, water molecules. The same interaction should also occur for cyt *c* adsorbed on 11-mercapto-1-undecanol films (MU) [38] for which the $E^{\circ\prime}$ value is 16 mV more positive than that on MP. This must be the result of the formation of different H-bond networks which are responsible for changes in the extent of the electrostatic interaction between the protein surface and the heme center.

Although the selective stabilization of the oxidized state of the adsorbed cyt *c* is expected to have an enthalpic origin on both SAMs, the decrease in $E^{\circ\prime}$ with respect to the solution conditions appears to be entropy driven (Table 1). In fact, immobilized cyt *c* features more negative $\Delta H^{\circ\prime}_{rc}$ and $\Delta S^{\circ\prime}_{rc}$ values as compared to the diffusing protein, with the latter contribution prevailing over the former (Table 1).

The following relationships hold:

$$E^{\circ\prime}_{ads} - E^{\circ\prime}_{sol} = -\frac{\Delta G^{\circ\prime}_{rc,ads}}{F} - \left(-\frac{\Delta G^{\circ\prime}_{rc,sol}}{F}\right) = -\frac{\Delta\Delta G^{\circ\prime}_{rc}}{F} \quad (3)$$

$$-\frac{\Delta\Delta G^{\circ\prime}_{rc}}{F} = -\frac{\Delta\Delta H^{\circ\prime}_{rc}}{F} + \frac{T\Delta\Delta S^{\circ\prime}_{rc}}{F} \quad (4)$$

where $E^{\circ\prime}_{ads}$ and $E^{\circ\prime}_{sol}$ are the redox potentials of adsorbed and freely diffusing bovine cyt *c*, respectively.

It can be demonstrated that the reduction entropy is almost entirely due to solvent reorganization effects, namely the reduction induces changes in the H-bonding network and ionic atmosphere within the hydration sphere of the protein [7, 8, 39]:

$$-\frac{\Delta\Delta G^{\circ\prime}_{rc}}{F} = -\frac{\Delta\Delta H^{\circ\prime}_{rc,solv} + \Delta\Delta H^{\circ\prime}_{rc,el}}{F} + \frac{T\Delta\Delta S^{\circ\prime}_{rc,solv}}{F} \quad (5)$$

where $\Delta\Delta H^{\circ\prime}_{rc,solv}$ is the change in $\Delta H^{\circ\prime}_{rc}$ due to the changes in the solvent organization induced by adsorption on the SAM, $\Delta\Delta H^{\circ\prime}_{rc,el}$ is the change in $\Delta H^{\circ\prime}_{rc}$ due to the interaction with the SAM and $\Delta\Delta S^{\circ\prime}_{rc,solv}$ is the change in $\Delta S^{\circ\prime}_{rc}$ due to the changes in the solvent organization induced by adsorption on the SAM (other contributions to $\Delta S^{\circ\prime}_{rc}$ are irrelevant and thus omitted [7, 8, 40]).

However, solvent reorganization phenomena are known to induce exactly compensatory enthalpy–entropy changes [40–42]:

$$\frac{\Delta\Delta H^{\circ\prime}_{rc,solv}}{F} = \frac{T\Delta\Delta S^{\circ\prime}_{rc,solv}}{F} \quad (6)$$

As a consequence, the observed decrease in $E^{\circ\prime}$ value can indeed be ascribed to the enthalpic term due to the electrostatic (MUA) or H-bond (MP) interactions between the protein and the SAM which stabilizes the oxidized form of the cyt *c*:

$$E^{\circ\prime}_{ads} - E^{\circ\prime}_{sol} = -\frac{\Delta\Delta G^{\circ\prime}_{rc}}{F} = -\frac{\Delta\Delta H^{\circ\prime}_{rc,el}}{F} \quad (7)$$

The values of $-\Delta\Delta H^{\circ\prime}_{rc,el}/F$ obtained on different SAMs are reported in Table 1. It is worth noting that the enthalpic stabilization follows the order MUA > MP > MU, according to the fact that cyt *c* interacts electrostatically with the anionic carboxylate groups of MUA through the surface lysines whereas H-bond interactions are involved with MP and MU. We note that 4-mercaptopyridine is only an acceptor of H-bonds, while 11-mercapto−1-undecanol acts both as donor and acceptor of H-bonds. This fact could justify the observed differences in the enthalpic stabilization effect.

As shown by Bowden et al., the $k_s$ value obtained using Laviron's method correspond to the kinetic constant for ET at zero driving force [12, 30, 43]. Therefore the Marcus equation for heterogeneous ET assumes the form [44]:

$$k_s = \nu_0 \exp[-\beta(r - r_0)] \exp\left(-\frac{\Delta G^{\#}}{RT}\right) = \nu_0 \exp[-\beta(r - r_0)] \exp\left(-\frac{\lambda}{4RT}\right) \quad (8)$$

where $\Delta G^{\#} = \frac{\lambda}{4}$.

Since the activation entropy in these systems is general negligible [30, 32, 45], $\Delta H^{\#}$ can be considered equal to $\Delta G^{\#}$ and obtained using the Arrhenius equation. Thus, $\lambda$ can be easily calculated. The $k_s$, $\Delta H^{\#}$ and $\lambda$ values determined for cyt *c* adsorbed on MUA and MP at pH = 7 in

5 mM $NaClO_4$ and 5 mM phosphate buffer are reported in Table 2. The rate constants $k_s$ are comparable, but the $\Delta H^{\#}$ values remarkably differ. In particular, cyt *c* on MP features a larger activation enthalpy and reorganization energy than on MUA. These data indicate that the nature of SAM influences both the reduction thermodynamics and kinetics of the ET process.

The distance (*r*) between the heme iron and the electrode surface for the protein adsorbed on MUA can be evaluated from the linearized Marcus equation:

$$\ln k_s = \ln v_0 - \beta(r - r_0) - \frac{\Delta G^{\#}}{RT} \quad (9)$$

using $v_0 = 6 \times 10^{12}\ s^{-1}$ [30], a $\beta$ value of 1 $Å^{-1}$ [30, 46, 47] and $r_0 = 3$ Å [12, 30, 44]. A *r* value of 26.8 ± 0.4 Å is obtained (the uncertainty on r has been calculated from the absolute errors affecting ln $k_s$ and $\Delta G^{\#}/RT$). Since the tunneling distance for the chains of MUA is about 19 Å [48, 49], the SAM surface should be 7.8 ± 0.4 Å from the heme iron, consistent with the heme edge being approximately 5–6 Å [27] below the protein surface.

In the case of cyt *c* adsorbed on MP, the medium separating the heme and the electrode surface cannot be considered homogeneous, as in the case of MUA, being formed by sections with remarkable different $\beta$ values. This fact requires the factorization of the first exponential term in the Marcus equation [10]:

$$k_s = v_0 \exp\left[-\sum_i (\beta_i r_i) + r_0\right] \exp\left(-\frac{\Delta G^{\#}}{RT}\right) \quad (10)$$

where $\beta_i$ and $r_i$ correspond to the tunneling factor and to the thickness of the *i*th medium, respectively, and the tunneling factor relative to $r_0$ is considered to be 1 $Å^{-1}$ [10, 30, 44]. In this case, at least four different media must be considered:

(1) the sulfur atom of 4-mercaptopyridine;
(2) the aromatic pyridine moiety;
(3) the interface region between the protein and the SAM surface, characterized by the presence of H-bond(s) and probably water molecule(s) responsible of the adsorption interaction of the (solvated) protein;
(4) the protein matrix between the heme and the cytochrome surface.

Each region is characterized by a specific $\beta$ value. The following $\beta_i$ and $r_i$ values were used, which were taken from literature values for similar molecular frames: $\beta_1 = 1.1\ Å^{-1}$ and $r_1 = 2$ Å [10, 50]; $\beta_2 = 0.4\ Å^{-1}$ and $r_2 = 5$ Å [10, 51]; $\beta_3 = 2\ Å^{-1}$ and $r_3$ is variable depending on the presence and number of solvation water molecules [10, 50]; $\beta_4 = 1.4\ Å^{-1}$ and $r_4 = 6$ Å (considering the most favorable and probable orientation with the surface lysines) [10, 50].

The linearized form of the Marcus equation can be used to evaluate the $r_3$ value:

$$\ln k_s = \ln v_0 - (\beta_1 r_1 + \beta_2 r_2 + \beta_3 r_3 + \beta_4 r_4 - r_0) - \frac{\Delta G^{\#}}{RT} \quad (11)$$

Assuming $v_0 = 10^{12}\ s^{-1}$ (as suggested for rigid spacers covalently linked to the electrode surface, as 4-mercaptopyridine) and $r_0 = 3$ Å [12, 30, 44, 52, 53], the thickness of the interface between protein and MP is 5.6 Å. This value is consistent with the presence of at least one water molecule at the interface between cyt *c* and MP. It is noteworthy that the reorganization energy $\lambda$ on MP is remarkably higher than that on MUA (0.36 eV vs. 0.25 eV, respectively) and that the value of $\lambda$ is prevalently determined by solvent reorganization effects [10]. These facts suggest that the water molecules at the interface between the protein and MP are somewhat more constrained than the others involved in the protein solvation. This fact would hinder solvent reorganization following the ET process thus increasing $\lambda$.

**Acknowledgment** This work was supported by the Ministero dell'Università e della Ricerca Scientifica e Tecnologica (MURST).

## References

1. Scott RA, Mauk GA (eds) (1996) Cytochrome *c*: a multidisciplinary approach. University Science Books, Sausalito CA
2. Messerschmidt A, Huber R, Poulos T, Wieghardt K (eds) (2001) Handbook of metalloproteins, vol 1. Wiley, Chichester
3. Armstrong FA, Hill HAO, Walton NJQ (1986) Rev Biophys 18:261
4. Armstrong FA (1990) Struct Bonding 72:137
5. Hill HAO, Hunt NI (1993) Methods Enzymol 227:501
6. Bond AM (1994) Inorg Chim Acta 226:293
7. Battistuzzi G, Borsari M, Sola M (2001) Antioxid Redox Signal 3:279
8. Battistuzzi G, Borsari M, Sola M (2001) Eur J Inorg Chem 2989
9. Armstrong FA, Wilson GS (2000) Electrochim Acta 45:2623
10. Fedurco M (2000) Coord Chem Rev 209:263
11. Xu J, Bowden EF (2006) J Am Chem Soc 128:6813
12. Tarlov MJ, Bowden EF (1991) J Am Chem Soc 113:1847
13. El Kasmi A, Wallace JM, Bowden EF (1998) J Am Chem Soc 120:225
14. Murgida DH, Hildebrandt PJ (2001) J Phys Chem B 105:1578
15. Heering HA, Wiertz FGM, Dekker C, de Vries J (2004) J Am Chem Soc 126:11103
16. Battistuzzi G, Borsari M, Bortolotti CA (2006) J Am Chem Soc 128:5444
17. Nahir TM, Bowden EF (1996) J Electroanal Chem 410:9
18. Clark RA, Bowden EF (1997) Langmuir 13:559
19. Tanimura R, Hill MG, Margoliash E, Niki K, Ohno H, Gray HB (2002) Electrochem Solid State Lett 5:E67–E70
20. Niki K, Hardy WR, Hill MG, Li H, Sprinkle JR, Margoliash E, Fujita K, Tanimura R, Nakamura N, Ohno H, Richards JH, Gray HB (2003) J Phys Chem B 107:9947

21. Imabayashi S, Mita T, Kakiuchi T (2005) Langmuir 2005 21:1470
22. Petrovic J, Clark RA, Yue H, Waldeck DH, Bowden EF (2005) Langmuir 21:6308
23. Collinson M, Bowden EF (1992) Langmuir 8:2552
24. Matsuda N, Santos JH, Takatsu A, Kato K (2003) Thin Solid Films 438:403
25. Habermuller L, Mosbach M, Schuhmann W (2000) Fresenius J Anal Chem 366:560
26. Northrup SH (1996) In: Scott RA, Mauk GA (eds) Cytochrome *c*: a multidisciplinary approach. University Science Books, Sausalito CA, pp 543
27. Louie GV, Brayer GD (1990) J Mol Biol 214:527
28. Chen X, Ferrigno R, Yang J, Whitesides GM (2002) Langmuir 18:7009
29. Collinson M, Bowden EF, Tarlov MJ (1992) Langmuir 8:1247
30. Song S, Clark RA, Bowden EF, Tarlov MJ (1993) J Phys Chem 97:6564
31. Yee EL, Cave RJ, Guyer KL, Tyma PD, Weaver MJ (1979) J Am Chem Soc 101:1131
32. Yee EL, Weaver MJ (1980) Inorg Chem 19:1077
33. Taniguchi VT, Sailasuta-Scott N, Anson FC, Gray HB (1980) Pure Appl Chem 52:2275
34. Koller KB, Hawkridge FM (1988) J Electroanal Chem 239:291
35. Laviron E (1979) J Electroanal Chem 101:19
36. Millo D, Bonifacio A, Ranieri A, Borsari M, Gooijer C, van der Zwan G (2007) Langmuir 23:4340
37. Leopold MC, Bowden EF (2002) Langmuir 18:2239
38. Gavioli G, Borsari M, Cannio M, Ranieri A, Volponi G (2004) J Electroanal Chem 564:45
39. Battistuzzi G, Loschi L, Borsari M, Sola M (1999) J Biol Inorg Chem 4:607
40. Battistuzzi G, Borsari M, Di Rocco G, Ranieri A, Sola M (2004) J Biol Inorg Chem 9:23
41. Grunwald E, Steel C (1995) J Am Chem Soc 117:5687
42. Liu L, Guo Q-X (2001) Chem Rev 101:673
43. Nahir TM, Clark RA, Bowden EF (1994) Anal Chem 66:2595
44. Marcus RA, Sutin N (1985) Biochim Biophys Acta 811:265
45. Weaver MJ (1979) J Phys Chem 13:1748
46. Becka AM, Miller CJ (1992) J Phys Chem 96:2657
47. Finklea HO, Hanshew DD (1992) J Am Chem Soc 114:3173
48. Hildebrand P, Murgida DH (2002) Bioelectrochem 55:139
49. Murgida DH, Hildebrand P (2001) J Phys Chem B 105:1578
50. Cheng J, Miller CJ (1997) J Phys Chem B 101:1058
51. Wenger OS, Leigh BS, Villahermosa RM, Gray HB, Winkler JR (2005) Science 307:99
52. Bendall DS (1996) Protein electron transfer. BIOS Scientific, Oxford
53. Moser CC, Dutton PL (1992) Biochim Biophys Acta 1101:171